Influence Of Ga Doping On The Structural, Optical And Electrical Properties Of $Ba_{0.6}Sr_{0.4}tio_3$ Thin Films

V. Eswaramoorthi, Sony Sebastian, R. Victor Williams

Abstract: The effects of Ga doping on the structural, optical and electrical properties of sol-gel routed $Ba_{0.6}Sr_{0.4}TiO_3$ thin films on quartz and silver coated quartz substrates have been investigated. XRD analysis indicates that the crystallite size decreases with increase in dopant concentration and the strain in the film is compressive in nature. SEM analysis reveals that the surface smoothness improves with dopant concentration. EDX analysis reveals the presence of gallium in the doped material. The dielectric constant and dielectric loss decrease with dopant concentration whereas the tunability and figure of merit increase with dopant concentration. The UV-Vis transmission spectrum analysis shows that the transmittance and the refractive index of the film decrease with dopant concentration. The band gap of the film increases with dopant concentration.

Keyword: BST, Dielectric properties, Optical properties, Structural properties, Sol-gel, Thin film, Tunability.

1 INTRODUCTION

In future, there might be a need for memory requirements with trillion bits stored on a stamp sized memory device [1]. The society is going to meet these growing demands with some novel materials possibly ferroelectric materials being one among them. Analysis of the current research indicates that ferroelectric RAM (FeRAM) is a good candidate for DRAM applications. The BaxSr1-xTiO3 thin film (BST) is one of the perovskite structures that has drawn the attention of the researchers because of its significant properties such as good stability, high dielectric constant, low dielectric loss and low leakage current [2]. Due to these properties, BST thin films have been widely used in variety of applications such as microwave devices, pyroelectric sensors, dynamic random access memory [3, 4] and optoelectronic devices [5-7]. BST is one of the most widely investigated materials for high **TUNABILITY.** But there are some constraints in achieving the high tunability which is accompanied by high loss tangent [8]. The reduction in dielectric loss in BST thin films is achieved through doping. The doped BST film is being explored mostly because of their use in next generation memory applications [9]. The oxygen vacancy existing in perovskite crystal structure acts as an intrinsic donor which can generate electron–hole pair [10], whereas the metals doped in BST film acts as an extrinsic donor (or) acceptor. Several metals were investigated as extrinsic dopant where the metal atoms can substitute onto A or B sites of ABO3 structure. The A or B substituted sites are relatively dependent on their ionic radii. The B site substituted metal ions can act as an extrinsic acceptor, such as Fe3+ [11, 12], Co3+ [13], Ni2+ [14], Cu2+ [15], Ca2+ [16]. The A site substituted metal ions can act as an extrinsic donor, such as Pr3+ [11], La3+ [17] and Nd3+ [18]. Some metal ions such as Dy3+ [17], Ho3+ [19], Sb3+ [20] and Er3+ [21] can substitute both A and B sites. BST thin films have been prepared by several techniques like metal organic chemical vapor deposition (MOCVD) [22], sputtering [23], pulsed laser deposition [24], chemical solution deposition [25] and sol-gel [26]. Among those techniques sol-gel is a simple and low cost technique because of its better homogeneity, large area deposition, precision stoichiometry control and convenience in processing. In the present work, the influence of Ga on Ba0.6Sr0.4TiO3 thin films was investigated as there are no reports available on Ga doped Ba0.6Sr0.4TiO3 thin films by sol-gel with different dopant concentrations. Hence, our work is to understand the effects due to Ga doping on structural, optical and electrical properties of Ba0.6Sr0.4TiO3 thin films.

- *Research Scholar, Department of Physics, St.Joseph's College, Tiruchirappalli-620002, Tamil Nadu, India, Mobile: 09952235383, E-mail: physicseswar@gmail.com*
- *Research Scholar, Department of Physics, St.Joseph's College, Tiruchirappalli-620002, Tamil Nadu, India, Mobile: 09446070044, E-mail: sonyseban303@gmail.com*
- *Corresponding Author: Associate Professor and Head, Department of Physics, St. Joseph's College, Tiruchirappalli-620002, Tamil Nadu, India, Mobile:09443650091, E-mail: rvwi@yahoo.com*

2 EXPERIMENTAL METHODS

The precursor solutions for both undoped and Ga doped $Ba_{0.6}Sr_{0.4}TiO_3$ thin films were prepared by sol-gel method. Barium acetate ($Ba(CH_3COO)_2$), strontium acetate ($Sr(CH_3COO)_2$), gallium (III) oxide (Ga_2O_3), titanium (IV) butoxide (Ti $(C_4H_9O)_4$) were used as starting materials. Glacial acetic acid and acetyl acetone were used as solvent and stabilizer. The solid state barium acetate and strontium acetate were taken in ratio 60:40 and dissolved into heated glacial acetic acid. A clear solution had been obtained. Few drops of acetyl acetone were added as stabilizer followed by the addition of suitable amount of titanium (IV) butoxide into the solution. Gallium (III) oxide with different concentrations ranging from 0, 0.5 and 1 mol % was added to the solution as a dopant precursor. The solution was sonicated for 2hours. Due to cross linking reaction the viscosity of the solution gradually increased. After 30 minutes the solution attained a suitable viscosity for coating. The Ga doped BST thin films were deposited on silver coated quartz and quartz substrates by spin coating technique at 5500 rpm for 60s. The coated films were annealed at 400ºC for 30 minutes to remove the organic volatiles and at 800ºC for 30 minutes to obtain crystallization. The crystal structure of the film was examined using X-ray diffraction (Rigaku MiniFlex 600) and surface

morphology of pure and doped BST thin films was analyzed by Scanning Electron Microscope (Carl Zeiss MA15 / EVO 18). The compositional analysis was carried out using Energy Dispersive X–ray spectrum. The optical transmission spectra of BST films were measured in the wavelength range of 190-1100 nm using UV-Visible spectrometer (Perkin elmer lambda 35). The optical parameters were calculated on the basis of the envelope method. The dielectric properties of the BST thin films were measured using Metal-Insulator-Metal (MIM) structured cell with LCR Bridge. Gold had been sputtered over the film as top electrode through shadow masking method. Silver had been used as bottom electrode.

3 Result and Discussion

3.1 XRD analysis

The deposited undoped and Ga doped BST thin films were subjected to XRD analysis for their phase identification. Figure 1 shows the XRD pattern of deposited undoped and Ga doped BST thin films. It is inferred from the XRD studies that the deposited thin films possess polycrystalline with cubic structure and the XRD peaks were compared with standard JCPDS Data Card (34-0411). The perovskite phase formed with the absence of secondary phase (derivatives of Ga) was shown in Fig.1.

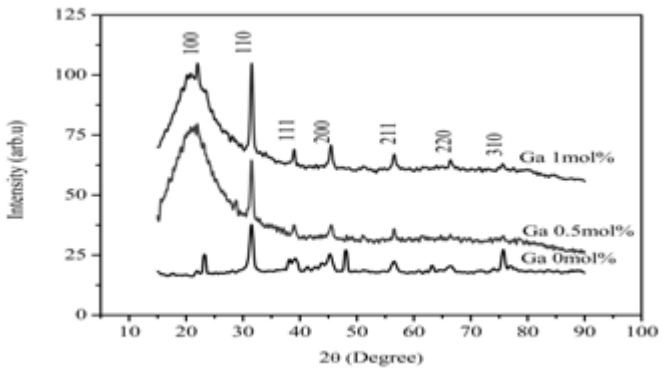

Fig. 1. *X-ray diffraction of BST thin films for different Ga concentrations.*

The X-ray pattern shows that there is no change in the intensity of peaks with dopant concentration. The lattice constant (a) of the samples were calculated. The effective ionic radius of Ga^{3+} ion (0.62Å) is slightly larger than Ti^{4+} (0.61Å), so it enters into B-sites and gets substituted in the place of Ti^{4+}ions. High temperature annealing in air can promote the lattice parameters to increase [27]. The films preheated at 400ºC and annealed at 800ºC may be responsible for the increase in lattice parameters. The increase in lattice parameters of Ga doped BST thin films were clearly observed as the 2θ peak shifted toward lower angle in compared with undoped BST thin films. The crystallite size and lattice strain of the deposited films were evaluated by using Williamson–Hall plots. W–H plots were drawn with sinθ in x-axis and βcosθ in the y-axis that was shown in Fig.2. From the linear fit of the data, the slope determines the lattice strain (ε) and the intercept determines the crystallite size (D) (Eq.1) [28]

$$\beta\cos\theta = \frac{0.9\lambda}{D} + 4\varepsilon\sin\theta \qquad (1)$$

Where β is the full width at half maximum of the diffraction peak at 2θ, λ is the X-ray wavelength, D is the average crystallite size and ε is the lattice strain experienced by the crystallites. The variation of lattice strain with crystallite size is shown in Fig. 2. The crystallite size of Ga doped BST thin films with (110) peak in the XRD patterns are listed in Table 1.

TABLE 1 *Calculated values of crystallite size, dislocation density, strain of BST thin films for various Ga dopant concentrations.*

BST Films (Ga doped)	2Theta (110) (°)	Calcd (Å)	JCPDS d (Å)	Crystallite size (D) nm	Dislocation density (δ) $\times 10^{15}$ m^{-2}	Strain (ε) $\times 10^{-3}$
0 mol %	31.49	2.838	2.803	25	2.29	-2.4641
0.5 mol %	31.47	2.840	2.803	20	2.35	-1.6410
1 mol %	31.43	2.84	2.803	18	2.41	-0.0014

From the table it is observed that the crystallite size decreases with increase in dopant concentration and the negative values of lattice strain indicates the compressive strain present in crystallites [29]. The dislocation density (δ) (Eq. 2) was determined using Williamson and Smallman's formula βcosθ in the y-axis that was shown in Fig.2. From the linear fit of the data, the slope determines the lattice strain (ε) and the intercept determines the crystallite size (D) (Eq.1) [28]

$$\beta\cos\theta = \frac{0.9\lambda}{D} + 4\varepsilon\sin\theta \qquad (1)$$

Where β is the full width at half maximum of the diffraction peak at 2θ, λ is the X-ray wavelength, D is the average crystallite size and ε is the lattice strain experienced by the crystallites. The variation of lattice strain with crystallite size is shown in Fig. 2. The crystallite size of Ga doped BST thin films with (110) peak in the XRD patterns are listed in Table 1. From the table it is observed that the crystallite size decreases with increase in dopant concentration and the negative values of lattice strain indicates the compressive strain present in crystallites [29]. The dislocation density (δ) (Eq. 2) was determined using Williamson and Smallman's formula

$$\delta = \frac{1}{D^2} \qquad (2)$$

Dislocation density increases with increase of the dopant concentration due to the strain in the film (Table 1). The dielectric loss decreases due to the increase of dislocation density.

3.2 Morphology and Compositional analysis

The morphological studies of the films were obtained using

SEM. Figure 3(a) and 3(b) shows the SEM micrographs of the films.

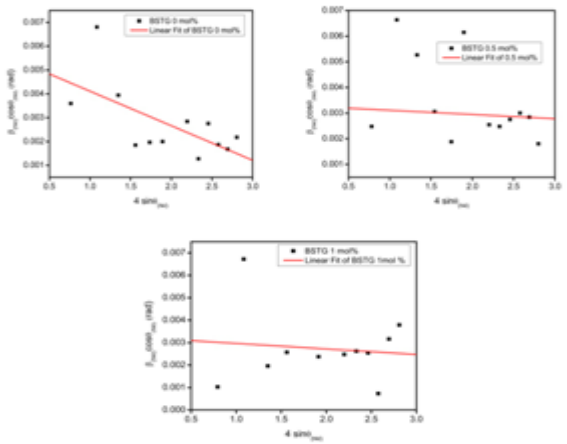

Fig. 2*. Williamson–Hall plots for Ga doped BST thin films.*

The SEM images indicate that surface smoothness of the film improves with dopant concentration. The cracks found in the film were due to the lattice mismatch between the film/substrate interfaces. The lattice mismatch is because of the thermal expansion coefficient of silver being lower than that of the film. The composition of the film was analyzed using energy dispersive X-ray spectrum (EDX) (Fig. 4(a), 4(b) and 4(c)). The EDX spectra of Ga doped BST thin films confirm the presence of barium, strontium, titanium and gallium. The percentage of elements present in the film is given in Table 2.

TABLE 2: *Compositional analysis of Ga doped BST thin films at various doping concentrations*

Sample code	Ga doped BST thin films		
	0 mol %	0.5 mol %	1 mol %
Element	Atomic %	Atomic %	Atomic %
O K	53.47	60.62	56.48
Si K	22.85	16.34	32.29
Ti K	4.78	5.82	3.81
Ga K	-	0.26	0.46
Sr L	2.15	3.77	3.13
Ag L	12.80	7.90	-
Ba L	3.94	5.29	3.83

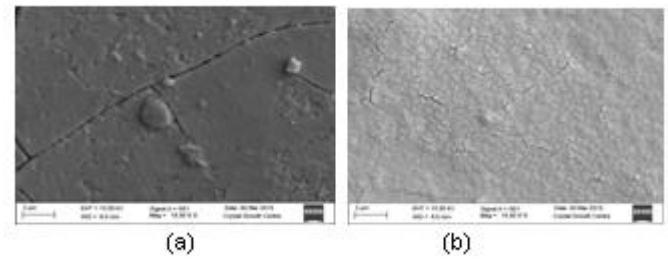

Fig. 3. (a*) SEM image of 0.5 mol% (b) 1 mol% Ga doped BST thin films.*

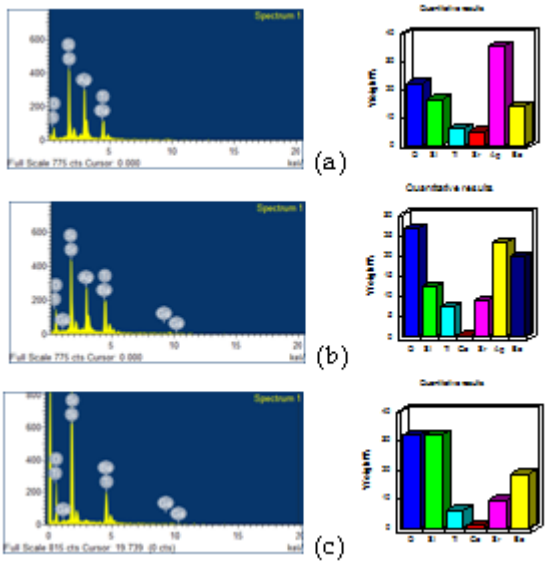

Fig. 4. EDX spectrum of (a) 0 mol% (b) 0.5 mol% (c) 1 mol% Ga doped BST thin films

3.3 Dielectric Properties

The dielectric constant of undoped and Ga doped BST thin films as a function of frequency is as shown in Fig.5(a). The figure shows that the dielectric constant decreases with frequency and dopant concentration. This decrease of dielectric constant is due to two reasons: (a) the dipoles which cannot follow the applied field. The higher value of the dielectric constant at low frequencies is due to the accumulation of charges at the grain boundaries and at the interfaces between the sample and electrodes (space- charge polarization), and (b) the decrease in dielectric constant is attributed to the decrease in grain size of the Ga-doped BST thin films. The decrease in grain size decreases the volume of polarization and increases the amount of low dielectric constant grain boundaries and/or induces more grain boundary defects per unit volume. The dielectric constant of 0, 0.5 and 1 mol % Ga doped BST thin films at 100 KHz for silver coated quartz were 1991, 1176 and 229 respectively.

The dielectric loss of Ga doped BST thin films as a function of frequency was shown in Fig.5(b). The figure shows that the dielectric loss decreases with the dopant concentration. The dielectric loss of 0, 0.5 and 1 mol % Ga doped BST thin films at 100 KHz were 0.63%, 0.43% and 0.22%. The reasons for the smaller dielectric loss of the Ga doped BST films are: (a) the Ga3+ ion attracts and neutralizes hopping electrons between the different titanium ions leading to the reduction of dielectric loss, and (b) as Ga (0.62Å) and Ti (0.61Å) have almost equal ionic radii, Ga3+ ions may occupy the B sites of Ti4+ in the ABO3 perovskite structure and behave as electron acceptor. The presence of acceptor ion prevent the reduction of Ti4+ to Ti3+ by neutralizing the donor action of the oxygen vacancies giving rise to reduction in dielectric loss [30]. In addition to this the dopant ion also neutralizes the electrons released from intrinsic vacancies that are generated due to high temperature annealing in the air atmosphere [31]. The decrease in electron concentration leads to lower dielectric loss as compared to the undoped film.

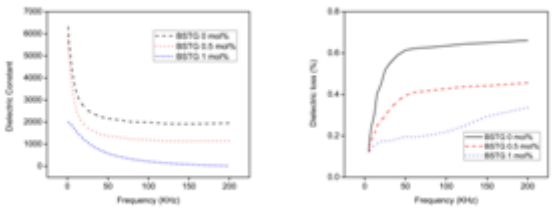

Fig. 5. *(a)Dielectric constant and (b) dielectric loss of BST thin films as a function of frequency with different dopant concentration*

3.4 Tunability of the Capacitance

Figure 6(a) shows the variation of capacitance at 100 KHz as a function of bias voltage for various Ga doped BST thin films. The measurements have been made at room temperature. It shows that the capacitance of the samples decreases nonlinearly with increasing voltage, which is in agreement with the literature [32]. The asymmetry of the capacitance reflects the influence of interfacial layers between the electrodes which should affect the polarization of the Ga doped BST thin films [33]. The tunability is determined by $(C_{max}-C_{min})/C_{max}$. where C_{max} and C_{min} are the values of capacitance at zero and maximum bias voltages respectively. The tunability of Ga doped BST thin films increases with the dopant concentration (Fig.6(b)). Acceptor type dopants generally improve the tunability property of BST thin films [34 - 35]. As Ga is an acceptor type dopant it increases the tunability of the BST thin films. Figure of merit (FOM) is a parameter frequently used to characterize the correlations between tunability and dielectric loss. FOM=(%tunability/%dielectric loss). The FOM value should be as high as possible for a design criterion of tunable devices [36]. Figure 6(c) shows that FOM increases with the dopant concentration. Based on the tunability and dielectric loss values of the Ga-doped BST thin films it can be concluded that the BST thin film is a potential candidate for tunable device applications.

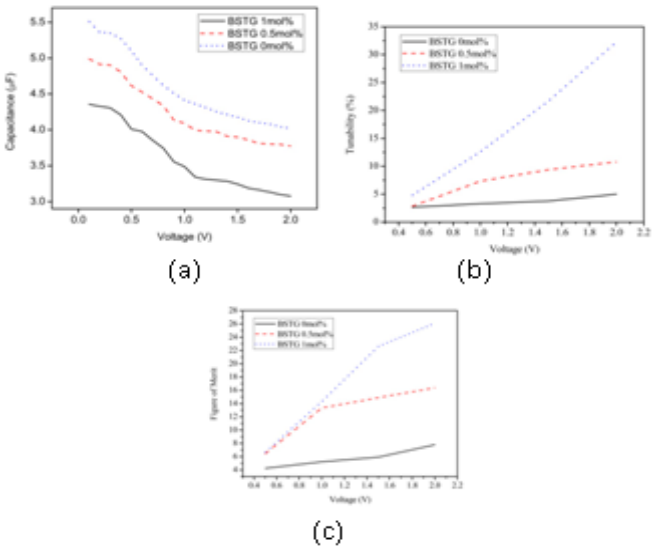

Fig. 6. (a)*Variation of capacitance at 100 KHz (b) Tunability (c) Figure of Merit as a function of bias voltage for Ga doped BST thin films.*

3.5 Transmittance and Band gap

The variation of transmittance of undoped and Ga doped BST thin films were shown in Fig.7(a). The undoped BST thin film has the high transparency in the visible region. The transparency of the film decreases with increase in dopant concentration. The absorption edges of the films were found to be 315, 331 and 331 nm for films with different Ga dopant concentration. The transmittance value for 0 mol%, 0.5 mol% and 1 mol% Ga doped BST thin films were 93%, 59% and 56% respectively. The decrease in transmittance is due to the development of micro crystallites that might lead to the scattering of light.

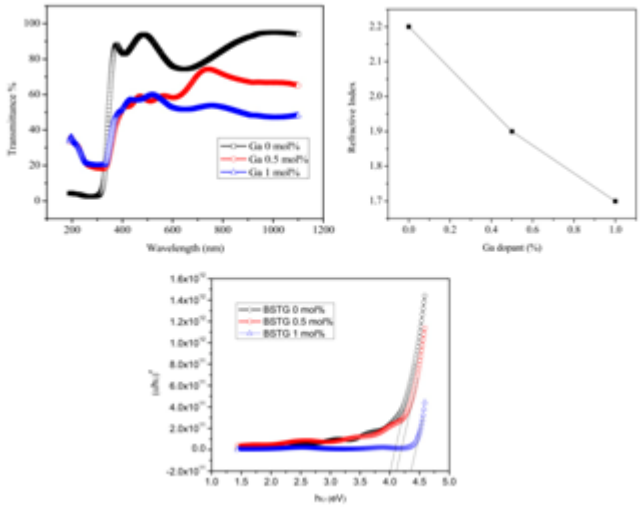

Fig. 7. (a) *Transmittance (b) Refractive Index (c) Band gap values of BST thin films as a function of Ga concentration.*

The optical band gap value can be determined from the Tauc's relation [26]

$$\alpha = \frac{A(h\nu - E_g)^n}{h\nu} \quad (3)$$

where A is a dimensional constant, Eg the optical band gap and n is the index representing the transition order. For a direct optical band gap, n = 2 and for an indirect optical band gap n = 1/2. The optical band gap was determined by extrapolating the linear portion of the plot relating $(\alpha h\nu)^2$ vs hν to the value α = 0. Figure 7(b) shows the refractive index of the film for various dopant concentrations calculated using swanepoel method. The refractive index decrease with dopant concentration is due to the increase of the band gap value. Figure 7(c) shows the band gap of the films for various dopant concentrations. The band gap energy increases with dopant concentration. The reduction of the intermediate energy levels within the band gap can be the reason for increase in optical band gap values. These reductions are due to the increase of structural formation into the lattice [37 - 38]. The band gap may vary due to the change in crystallite size. Crystallite size decreases with dopant concentration so that band gap increases [39]. The band gap values for 0 mol%, 0.5 mol% and 1mol% Ga doped BST thin films are 4, 4.1 and 4.3 respectively.

4 CONCLUSION

Ga doped $Ba_{0.6}Sr_{0.4}TiO_3$ thin films were prepared by sol-gel method on quartz and silver coated quartz substrates. The XRD pattern confirms the structure of the film as polycrystalline in nature with cubic crystal system. The SEM micrographs show that the surface morphology varies with dopant concentration. EDX analysis establishes the fact that Ga replaces Ti in the perovskite structure. The dielectric constant and dielectric loss decreases with dopant concentration. The increase of dopant concentration leads to drastic change in the tunability and figure of merit. The tunability increases from 10% to 32.5% with the increase of 0.5 mol% of Ga. The refractive index of the film decreases from 2.2 to 1.7 with increase of the dopant concentration. The band gap value lies in the range between 4.0 - 4.3 eV. The above results suggest that Ga doped BST thin films can be used for tunable device applications.

REFERENCES

[1] P.Ball, High density memory: A switch in time, Nature,Vol 445, pp. 362–363, 2007.

[2] B.Hou, Y.Xu, D.Wu, Y.Sun, Preparation and characterization of single-crystalline barium strontium titanate nanocubes via solvothermal method, Powder.Technol. Vol 170, pp. 26–30, 2006.

[3] C.Mao, X.Dong, T.Zeng, H.Chen, F.Cao, Nonhydrolytic sol–gel synthesis and dielectric properties of ultrafine-grained and homogenized Ba0.70Sr0.30TiO3. Ceram. Int. Vol 34, pp. 45–49, 2008.

[4] Y.B.Khollam, S.B.Deshpande, H.S.Potdar, S.V.Bhoraskar, S.R.Sainkar, S.K.Date, Simple oxalate precursor route for the preparation of barium–strontium titanate: Ba1−xSrxTiO3 powders. Mater.Charact. Vol 54, pp. 63–74, 2005.

[5] F.M.Pontes, C.D.Pinheiro, E.Longo, E.R.Leite, S.R.De Lazaro, R.Magnani, P.S.Pizani, T.M. Boschi, F.Lanciotti, Theoretical and experimental study on the photoluminescence in BaTiO3 amorphous thin films prepared by the chemical route. J. Lumin. Vol 104, pp. 175–185, 2003.

[6] F.M.Pontes, E.Longo, E.R.Leite, E.J.H.Lee, J.A.Varela, P.S.Pizani, C.E.M.Campos, F.Lanciotti, V.Mastellaro, C.D.Pin heiro, Photoluminescence at room temperature in amorphous SrTiO3 thin films obtained by chemical solution deposition, Mater.Chem.Phys. Vol 77, pp. 598–602, 2003.

[7] J.Wang, T.Zhang, R.Pan, Z.Ma, J.Wang, Influence of Tm-doping on microstructure and luminescence behavior of barium strontium titanate thick films. Appl.Surf.Sci. Vol 258, pp. 3283–3288, 2012

[8] M.F.Hu, Y.Zhuo, S.X.Wang, Y.Tian, Study on dielectric and tunable properties of Cr-doped Ba0.6Sr0.4TiO3 thin films by rf sputtering, J.Mater.Sci. Vol 43, pp. 3162–3165, 2008.

[9] D.Gulwade, P.Gopalan, Diffuse phase transition in La and Ga doped barium titanate, Solid State Commui.Vol 146, pp. 340–344, 2008.

[10] R.Moos, K.H.Hardtl, Defect Chemistry of Donor-Doped and Undoped Strontium Titanate Ceramics between 1000° and 1400°C. J. Am. Ceram. Soc.Vol 80, pp. 2549–2562, 1997.

[11] X.Zhou, H.Gewein, M.Sazegar, A.Giere, F.Paul, R.Jakoby, J.Binder, J.Hauelt, Characterization of metal (Fe, Co, Ni, Cu) and fluorine codoped barium strontium titanate thick-films for microwave applications, J. Electroceram. Vol 24, pp. 345–354, 2010.

[12] M.T.Buscagila, V. Buscagila, M.Vivani, P.Nanni, M.Hanuskova, Influence of foreign ions on the crystal structure of BaTiO3, J. Eur. Ceram. Soc. Vol 20, pp. 1997–2007, 2000.

[13] L.Gao, J.Zhai, X.Yao, The influence of Co doping on the dielectric, ferroelectric and ferromagnetic properties of Ba0.70Sr0.30TiO3 thin films, Appl. Surf. Sci. Vol 255,pp. 4521–4525, 2009.

[14] V.Eswaramoorthi, R.V.Williams, Structural, optical and electrical properties of sol–gel derived (Ba0.6Sr0.4)(NixTi1−x)O3 thin films, Ceram. Int. Vol 41, pp. 2434–2438, 2015.

[15] H.T.Langhammer, T.Muller, R.Bottcher, H.P. Abichut Crystal structure and related properties of copper-doped barium titanate ceramics, Solid.State.Sci. Vol 5, pp. 965–971, 2003.

[16] Y.Li, X.Yao, L.Zhang, Dielectric properties and microstructure of magnesium-doped Ba1+k(Ti1−xCax)O3−x+k ceramics, Ceram. Int. Vol 30, pp. 1283–1293, 2004.

[17] P.Yongping, Y.Wenchu, C.Shoutian, Influence of Rare Earths on Electric Properties and Microstructure of Barium Titanate Ceramics, J. Rare Earth. Vol 25, pp. 154–157, 2007.

[18] Z.Yao, H.Liu, Y.Liu, Z.Wu, Z.Chen, Y.Liu, M.Cao, Structure and dielectric behavior of Nd-doped BaTiO3 perovskites, Mater. Chem. Phys. Vol 109, pp. 475–481, 2008.

[19] T.Zhang, J.Wang, J.Jiang, R.Pan, B.Zhang, Microstructure and photoluminescence properties of Ho-doped (Ba,Sr)TiO3 thin films, Thin Solid Films Vol 515, pp. 7721–7725, 2007.

[20] E.Brzozowski, A.C.Caballero, M.Villegas, M.S.Castro, J.F.Fernandez, Effect of doping method on microstructural and defect profile of Sb–BaTiO3, J. Eur. Ceram. Soc. Vol 26, pp. 2327–2344, 2006.

[21] S.Y.Kuo, W.F.Hsieh. Structural and optical properties of erbium-doped Ba0.7Sr0.3TiO3 thin films, J. Vacc.

Sci. Technol. A Vol 23, pp. 768–772, 2005.

[22] T.S.Seo,Y.N.Oh, E.S.Choi, S.G.Yoon, The Tunable Characteristics of Ni-Doped (Ba0.5Sr0.5)TiO3 Thin Films Deposited onto MOCVD-(Ba0.5Sr0.5)RuO3 Conductive Interfacial Layers, Integer. Ferroelec. Vol 49, pp. 93–102, 2002.

[23] L.Song, Y.Chen, G.Wang, L.Yang, T.Li, F.Gao, X.Dong, Dielectric properties of La/Mn codoped Ba0.63Sr0.37TiO3 thin films prepared by RF magnetron sputtering, Ceram. Int. Vol 40, pp. 12573-12577, 2014.

[24] S.Yu, L.Li, N.Zhang, H.Dong, D.Xu, W.Zhang, Bi1.5Mg1.0Nb1.5O7/Ba0.6Sr0.4TiO3 bilayer thin films prepared by pulsed laser deposition, J. Alloy. Compd. Vol 612,pp. 26–29, 2014.

[25] Irzman, H.Darmasetiawan, H.Hardhienata, M.Hikam, P.Arifin, S.N.Jusoh, S.Taking, Z.Jamal, M.A.Idris, Surface roughness and grain size characterization of annealing temperature effect for growth gallium and tantalum doped Ba0.5Sr0.5TiO3 thin film, Atom Indones. Vol 35, pp. 57–67, 2009.

[26] J.C.Tauc, Amorphous and Liquid Semiconductor. Plenum press, Newyork, 1974.

[27] J.D. Cui, G.X. Dong, Z.M. Yang, J. Du, Low dielectric loss and enhanced tunable properties of Mn-doped BST/MgO composites, J. Alloy. Compd. Vol 490, pp. 353–357, 2010.

[28] R. Suriakarthick , V. Nirmal Kumar , R. Indirajith , T.S. Shyju ,R. Gopalakrishnan, Photochemically deposited and post annealed copper indium disulphide thin films, Superlattice. Microst. Vol 75, pp. 667–679, 2014.

[29] W.Chang, C.M.Gilmore, W.J.Kim, J.M.Pond, S.W.Kirchoefer, S.B.Qadri, D.B.Chirsey, J.S.Horwit, Influence of strain on microwave dielectric properties of (Ba,Sr)TiO3 thin films, J. Appl. Phys. Vol 87, pp. 3044–3049, 2000.

[30] X. Liang, W. Wu, Z. Meng, Dielectric and tunable characteristics of barium strontium titanate modified with Al2O3 addition, Mater Sci Eng B, Vol 99, pp. 366–369, 2003.

[31] S.Y. Lee, T.Y. Tseng (2002) Electrical and dielectric behavior of MgO doped Ba0.7Sr0.3TiO3 thin films on Al2O3 substrate, Appl. Phys. Lett. Vol 80, pp. 1797–1799, 2002.

[32] A. Khalfallaoui, G. Velu, L. Burgnies, J. C. Carru, Characterization of doped BST thin films deposited by sol-gel for tunable microwave devices, IEEE T. Ultrason. Ferr. Vol 57, pp. 1029–1033, 2010.

[33] S. W. Jiang, B. Jiang, X. Z. Liu, and Y. R. Li, Laser deposition and dielectric properties of cubic pyrochlore bismuth zinc niobate thin films, J. Vac. Sci. Technol. A Vol 24, pp. 261–263, 2006.

[34] J.K. Kim, S.S. Kim,W.J. Kim, T.G. Ha, I.S. Kim, J.S. Song, R. Guo, A.S. Bhalla, Improved ferroelectric properties of Cr-doped Ba0.7Sr0.3TiO3 thin films prepared by wet chemical deposition, Mater Lett. Vol 60, pp. 2322–2325, 2006.

[35] Y. Ye, T. Guo, Dielectric properties of Fe-doped Ba0.65Sr0.35TiO3 thin films fabricated by the sol–gel method, Ceram. Int. Vol 35, pp. 2761–2765, 2009.

[36] S. Y. Lee, B. S. Chiou, H. H. Lu, Improving dielectric loss and enhancing figure of merit of Ba0.5Sr0.5Ti0.95Mg0.05O3 thin films doped by aluminum, Mater. Chem. Phys. Vol 108, pp. 55-60, 2008.

[37] J.C. Sczancoski, L.S. Cavalcante, T. Badapanda, S.K. Rout, S. Panigrahi, V. R. Mastelaro, J.A. Varela, M.S. Li, E. Longo, Structure and optical properties of [Ba1–xY2x/3](Zr0.25Ti0.75)O3 powders, Solid State. Sci. Vol 12, pp. 1160–1167, 2010.

[38] E.A.V. Ferri, J.C. Sczancoski, L.S. Cavalcante, E.C. Paris, J.W.M. Espinosa, A.T. de Figueiredo, P.S. Pizani, V.R. Mastelaro, J.A. Varela, E. Longo, Photoluminescence behavior in MgTiO3 powders with vacancy/distorted clusters and octahedral tilting, Mater. Chem. Phys. Vol 117, pp. 192–198, 2009.

[39] P.K. Sharma, G. L. Messing, D. K. Agarwal, Structural, ultraviolet-shielding, dielectric and ferroelectric properties of Ba1−xSrxTiO3 (x=0.35) thin films prepared by sol-gel method in presence of pyrrole, Thin solid films Vol 491, pp. 204–211, 2005.